

# <sup>13</sup>C Spin–Lattice Relaxation Times and NOE Related Studies of Hydroxyl-Terminated Polybutadiene (HTPB)

M. Z. Kassaei,\* H. Heydari, M. Hattami, and A. Fazli Nia

Department of Chemistry, University of Tarbiat Modarres, P.O. Box 14155-4838, Tehran, Iran

Received March 17, 2003; Revised Manuscript Received June 3, 2003

**ABSTRACT:** Hydroxyl-terminated polybutadiene, HTPB, carbon-13 spin–lattice ( $T_1$ ) and nuclear Overhauser effect (NOE) relaxations data, obtained as a function of temperature (–50 to +70 °C), in CDCl<sub>3</sub>, suggest that a log  $\chi^2$  distribution model is the most appropriate, in describing HTPB chain segmental motions. The local segmental motions are the major sources of relaxations, for the HTPB protonated carbons. The relaxation data show the chain segmental motions taking place in very short time intervals (on the order of tenth of a nanosecond). The activation energies of such conversions, from one conformer to another, are found to be on the order of kilojoules.

## Introduction

Hydroxyl-terminated polybutadiene, HTPB, is used extensively as a polymeric binder and is of considerable interest.<sup>1–2</sup> Recently, efforts are devoted to the study of dynamics of such polymers.<sup>3–10</sup> This is often done through the determination of <sup>13</sup>C NMR relaxation parameters.<sup>11–32</sup> The main advantage of this spectroscopic technique is providing a detailed analysis of molecular motions at the atomic levels. Several reviews are available which describe the various models developed for the interpretation of nuclear spin relaxation data of polymers.<sup>33–35</sup> As a model for molecular motion, the asymmetric log  $\chi^2$  distribution is useful at describing and quantifying the dynamics of polymers and polymer solutions.<sup>36–42</sup> The goal of this research is to obtain insights into the chain local motions of HTPB. Hence, the measurements, of the variable temperature (–50 to +70 °C) <sup>13</sup>C relaxation parameters of HTPB in CDCl<sub>3</sub> are presented. The relaxation data are interpreted in terms of chain local motions. This is using three dynamic models: (1) random isotropic tumbling, (2) log  $\chi^2$  distribution, and (3) modified log  $\chi^2$  distribution model. Among these, the log  $\chi^2$  distribution of Schaefer<sup>36</sup> appears to be the most appropriate in describing the chain segmental motions of HTPB.

## Theoretical Background

<sup>13</sup>C spin–lattice relaxation times,  $T_1$ , and nuclear Overhauser effects, NOE, are often used for studying the molecular dynamics of polymer chains.<sup>2–42</sup> These relaxations often arise from intermolecular dipole–dipole interactions. Practically for <sup>13</sup>C relaxations, only <sup>13</sup>C–<sup>1</sup>H nuclear dipoles are considered.  $T_1$  and NOE obtained from a <sup>13</sup>C NMR experiment can be expressed as follows<sup>13,31</sup>

$$\frac{1}{T_1} = NQ[J(\omega_H - \omega_C) + 3J(\omega_C) + 6J(\omega_H + \omega_C)] \quad (1)$$

$$\text{NOE} = 1 + \frac{\gamma_H}{\gamma_C} \left[ \frac{6J(\omega_H + \omega_C) - J(\omega_H - \omega_C)}{J(\omega_H - \omega_C) + 3J(\omega_C) + 6J(\omega_H + \omega_C)} \right] \quad (2)$$

\* Corresponding author. Fax: +98-21-8006544. E-mail: Kassaei@Modares.ac.ir or drkassaei@yahoo.com.

where

$$Q = \frac{1}{10} \left( \frac{\mu_0}{4\pi} \right)^2 \gamma_H^2 \gamma_C^2 \hbar^2 r_{CH}^{-6} \quad (3)$$

$\gamma_C$  and  $\gamma_H$  are the magnetogyric ratios of <sup>13</sup>C and <sup>1</sup>H nuclei, respectively.  $\mu_0$  is the vacuum magnetic permeability.  $\hbar$  equals  $h/2\pi$ , where  $h$  is Planck's constant.  $N$  is the number of protons.  $r_{CH}$  is the <sup>13</sup>C–<sup>1</sup>H distance.  $\omega_C$  and  $\omega_H$  are <sup>13</sup>C and <sup>1</sup>H resonance frequencies, respectively.  $J(\omega)$  is the spectral density function defined by:

$$J(\omega) = \int_{-\infty}^{+\infty} G(t) e^{i\omega t} dt \quad (4)$$

This is obtained by the Fourier transformation of the correlation function,  $G(t)$ , derived on the basis of specific models for polymer motions.<sup>4</sup>

The three motional models considered in this manuscript are as follows.

**(1) Random Isotropic Tumbling Model.** The rotational correlation time,  $\tau_C$ , may be approximately considered as the time required for the <sup>13</sup>C–<sup>1</sup>H vector to move through one radian. In the simple random isotropic tumbling model, the correlation function  $G(t)$ , is a single-exponential function decaying with  $\tau_C$ :

$$G(t) \cong \exp(-t/\tau_C) \quad (5)$$

Substitution of eq 5 into eq 4 and integration yields

$$J(\omega) \cong \frac{\tau_C}{1 + \omega^2 \tau_C^2} \quad (6)$$

**(2) The log  $\chi^2$  Distribution Model.** The log  $\chi^2$  distribution model, is reported by Schaefer.<sup>36</sup> It is very useful in describing and quantifying the dynamics of polymers and polymer solutions.<sup>11,33,36–42</sup> Accordingly, the spectral density function, appearing in  $T_1$  and NOE equations, is expressed in terms of a correlation time distribution. This is described by two parameters:  $p$  (width of the distribution) and  $\bar{\tau}$  (mean correlation time of the distribution). These occur in the spectral density

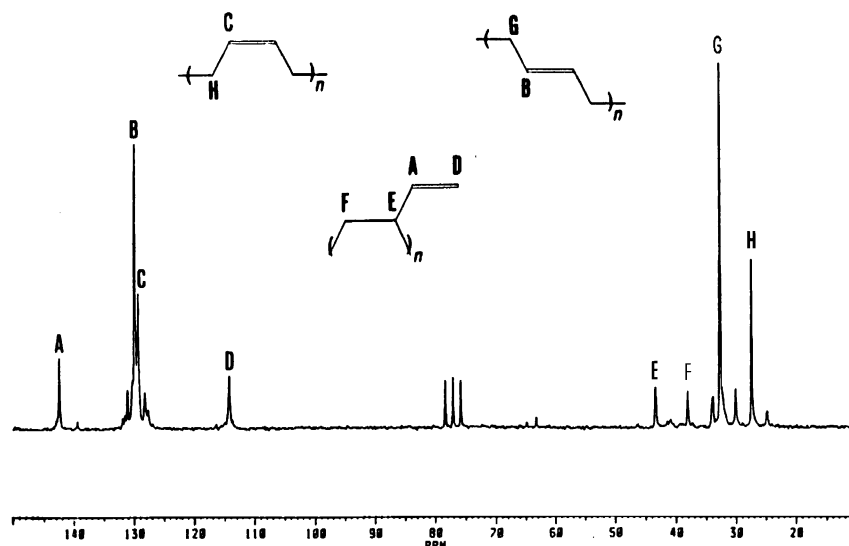


**Figure 1.** 25 MHz  $^{13}\text{C}$  NMR spectrum of 30% (w/v) hydroxyl-terminated polybutadiene (HTPB) in  $\text{CDCl}_3$  (with peak assignments) at room-temperature recorded by Bruker AC100 FTNMR.

function given by<sup>36</sup>

$$J(\omega) = \int_0^\infty \frac{\bar{\tau} G(s)(b^s - 1) ds}{(b - 1) \left[ 1 + \omega^2 \bar{\tau}^2 \left( \frac{b^s - 1}{b - 1} \right)^2 \right]} \quad (7)$$

where

$$G(s) ds = \frac{1}{\Gamma(p)} (ps)^{p-1} e^{-ps} p ds \quad (8)$$

This is a normalized distribution function.  $\Gamma(p)$  is the gamma function of  $p$  and represents a normalization factor.  $S$  is equal to  $\log_b[1 + (b - 1)\tau_C]$ .  $b$  is set at 1000.  $\bar{\tau}$  and  $p$  are calculated from experimental values of  $T_1$  and NOE.

**(3) Modified  $\log \chi^2$  Distribution Model.** O'Connor and Blum<sup>11,20,41,42</sup> state that the use of the  $\log \chi^2$  distribution may occasionally yield parameters which should not be compared from one system to another. They suggest that for some cases, a proper comparison can be made with the application of a correction factor. Also, the parameter  $\bar{\tau}$ , previously interpreted as the mean correlation time,<sup>41</sup> is considered not to be the true mean but rather a scaling factor which can be related to the true mean as follows:

$$\bar{\tau}_{\text{mod}} = \bar{\tau} \frac{\left( \frac{p}{p - \ln b} \right)^p - 1}{b - 1} \quad (9)$$

where  $\bar{\tau}_{\text{mod}}$  is correlation time. This is according to the modified  $\log \chi^2$  distribution.  $\bar{\tau}$  is the correlation time on the basis of the original  $\log \chi^2$  model.

## Experimental Section

**Materials.** The HTPB sample used in this study is obtained from Aldrich, with  $\bar{M}_n = 2900$ ,  $\bar{M}_w = 6100$ , functionality = 2.0,  $\bar{D}_p = 53$ ,  $[\eta] = 1.6$  dL/g at 25 °C, and cis/trans/vinyl ratio = 20/60/20.

**NMR Experiments.** The polymer is studied at 30% w/v in  $\text{CDCl}_3$ . A relatively high concentration of the polymer is used in order to achieve a better signal/noise (S/N) ratio.  $T_1$  and NOE values are measured using JEOL JNM-EX90A spectrometer operating at 22.6 MHz for the carbon nucleus. The sample temperature is regulated to  $\pm 1$  °C. Protons are

decoupled throughout  $^{13}\text{C}$  NMR experiments. To obtain a higher degree of precision, flip angle calibration is done. At 22.6 MHz the pulse width of  $90^\circ$  is found to be 10  $\mu\text{s}$ . All NMR experiments are performed on undegassed samples.

The standard inversion recovery method (PD- $\pi$ - $\tau$ - $\pi/2$ -AT), is used for  $^{13}\text{C}$ - $T_1$  measurements. This is with a pulse delay time, PD, longer than 5 times of the highest  $T_1$ . An initial estimate of the  $T_1$  values is obtained from preliminary experiments. The data acquisition time, is kept constant at 1 s. A total of 50 transients are accumulated for each set of 13 arrayed  $\tau$  values. These range from 0.001 to 20 s. Values of  $T_1$  obtained have an rms uncertainty of less than 5%.

NOE relaxations are measured by the comparison of  $^{13}\text{C}$  signal intensities of NOE retained vs. NOE suppressed spectra. Pulse delays of 10 times  $T_1$  are employed. Each NOE value is an average of two different measurements. All the relaxation data,  $T_1$  and NOE, are measured as a function of temperature in the range of -50 to +70 °C. These are with 10 °C increments.

**Numerical Analysis.** A Turbo Pascal program is written for this study which includes: isotropic,  $\log \chi^2$  and modified  $\log \chi^2$  motional models.<sup>2,43</sup> Inputs of this program are experimental  $T_1$  and NOE values. Outputs include:  $\tau_C$ ,  $\bar{\tau}$ ,  $\bar{\tau}_{\text{mod}}$ ,  $p$ ,  $T_1$ (calculated), and NOE(calculated). Minimum relative deviation between  $T_1$ (observed) vs.  $T_1$ (calculated) as well as NOE-(observed) vs NOE(calculated) is set at 1% of the corresponding values.

## Results

The  $^{13}\text{C}$  NMR spectrum of HTPB, along with its peak assignments, is illustrated in Figure 1. The experimental  $^{13}\text{C}$   $T_1$  and  $^{13}\text{C}\{^1\text{H}\}$  NOE values of HTPB, as a function of temperature, are listed in Table 1. The calculated activation energies for reorientation of HTPB carbon atoms via three dynamic models: isotropic tumbling,  $\log \chi^2$  distribution and modified  $\log \chi^2$  distribution are summarized in Table 2. An inversion recovery (180- $\tau$ -90) stacked plot of HTPB is shown in Figure 2. This is just a sample (out of  $2 \times 13$  obtained). Plots of experimental  $^{13}\text{C}$   $T_1$  and  $^{13}\text{C}\{^1\text{H}\}$  NOE values of protonated carbons of HTPB, as a function of temperature, are shown in Figure 3. Logarithms of correlation times as a function of temperature are presented in Figure 4 which is used for  $E_a$  calculations. These are calculated using: (a) isotropic tumbling model,  $\tau_C$ , (b)  $\log \chi^2$  distribution model,  $\bar{\tau}$ , and (c) modified  $\log \chi^2$  distribution model,  $\bar{\tau}_{\text{mod}}$ . Calculated  $p$  values for pro-

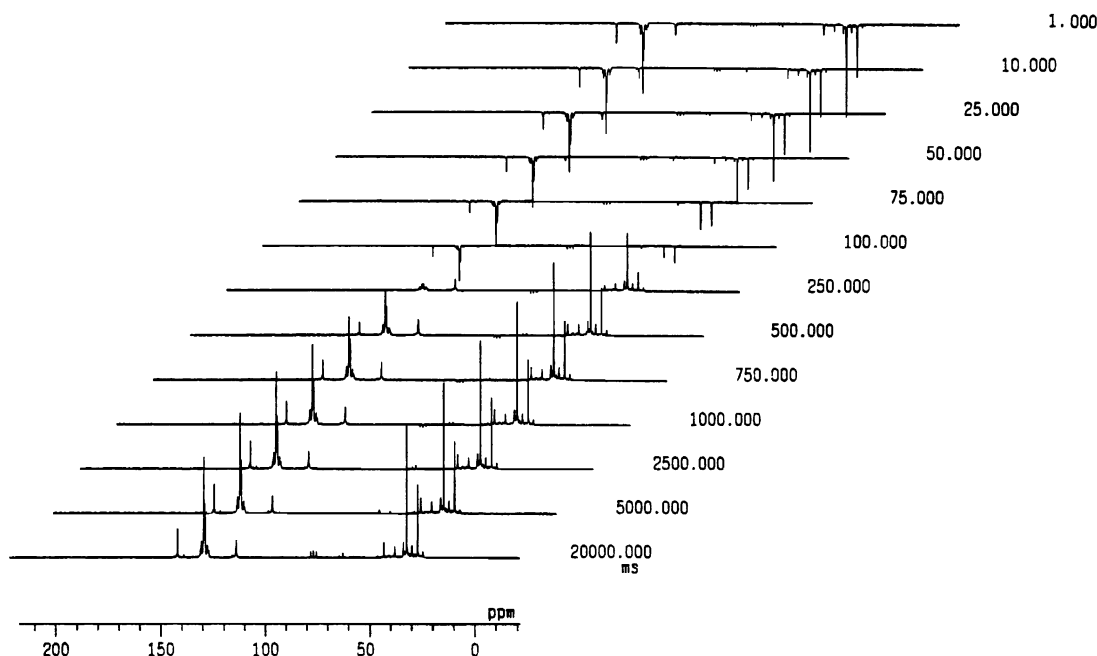


**Figure 2.** Sample inversion recovery <sup>13</sup>C NMR spectra of 30% (w/v) hydroxyl-terminated polybutadiene (HTPB) in CDCl<sub>3</sub> recorded by 22.6 MHz JEOL EX90 FTNMR.

**Table 1.** <sup>13</sup>C Spin–Lattice Relaxation Times (*T*<sub>1</sub>, ms) and NOE Values (in Parentheses) of Protonated Carbons of HTPB in CDCl<sub>3</sub> as a Function of Temperature in a 22.63 MHz Magnetic Field

<sup>13</sup> C NMR peak <sup>a</sup> (ppm)	<i>T</i> <sub>1</sub> , ms (NOE)													
	−50 °C	−40 °C	−30 °C	−20 °C	−10 °C	0 °C	10 °C	20 °C	30 °C	40 °C	50 °C	60 °C	70 °C	
A (142.2)	172 (2.33)	180 (2.24)	185 (2.26)	199 (2.29)	229 (2.34)	244 (2.40)	364 (2.50)	612 (2.61)	807 (2.72)	1067 (2.81)	1240 (2.82)	1405 (2.86)	1550 (2.89)	
B (129.6)	169 (2.02)	175 (2.04)	183 (2.07)	198 (2.11)	225 (2.15)	257 (2.21)	356 (2.38)	583 (2.57)	775 (2.69)	877 (2.73)	1150 (2.78)	1280 (2.81)	1395 (2.84)	
C (129.1)	149 (1.94)	163 (1.97)	178 (2.00)	197 (2.04)	219 (2.09)	236 (2.15)	312 (2.30)	548 (2.46)	657 (2.48)	863 (2.62)	973 (2.65)	1080 (2.67)	1210 (2.71)	
D (114.1)	68 (2.01)	75 (2.04)	83 (2.06)	92 (2.11)	103 (2.17)	115 (2.26)	138 (2.45)	208 (2.60)	258 (2.82)	434 (2.95)	486 (2.96)	565 (2.97)	670 (2.97)	
E (43.2)	64 (1.91)	69 (1.92)	75 (1.97)	83 (2.03)	90 (2.08)	99 (2.16)	208 (2.29)	353 (2.48)	349 (2.41)	441 (2.42)	587 (2.43)	692 (2.45)	808 (2.46)	
F (37.9)	36 (2.21)	37 (2.22)	39 (2.23)	42 (2.25)	44 (2.39)	47 (2.42)	95 (2.44)	156 (2.55)	178 (2.57)	200 (2.61)	299 (2.66)	401 (2.69)	529 (2.72)	
G (32.4)	107 (2.02)	109 (2.05)	114 (2.10)	118 (2.16)	121 (2.24)	126 (2.32)	175 (2.42)	276 (2.56)	338 (2.58)	457 (2.62)	549 (2.63)	672 (2.65)	835 (2.67)	
H (27.2)	149 (2.27)	153 (2.28)	156 (2.29)	160 (2.30)	165 (2.31)	172 (2.33)	234 (2.34)	362 (2.43)	544 (2.57)	635 (2.59)	790 (2.66)	905 (2.69)	1180 (2.73)	

<sup>a</sup> See Figure 1.

**Table 2.** Activation Energies of Protonated Carbons of HTPB Calculated from <sup>13</sup>C NMR Relaxation Data by Three Dynamic Models: Isotropic Tumbling, log  $\chi^2$  Distribution and Modified log  $\chi^2$  Distribution

<sup>13</sup> C NMR peak <sup>a</sup> (ppm)	<i>E</i> <sub>a</sub> (kJ/mol)		
	isotropic tumbling	log $\chi^2$ distribution	modified log $\chi^2$ distribution
A (142.2)	13.60	14.89	39.14
B (129.6)	12.99	15.92	55.41
C (129.1)	12.53	23.22	93.80
D (114.1)	13.02	12.31	73.16
E (43.2)	15.20	35.76	33.34
F (37.9)	15.33	25.52	17.36
G (32.4)	11.75	15.90	79.21
H (27.2)	11.89	13.22	59.56

<sup>a</sup> See Figure 1.

tonated carbons of HTPB, as a function of temperature, are shown in Figure 5.

## Discussion

In modeling the dynamics of HTPB, two types of motions are considered: (a) the overall tumbling of the entire chain, or large segments of HTPB, and (b) segmental backbone rearrangements.

These sources of motional behavior are assumed to be independent. Thereupon, the composite autocorrelation functions are written as a product of the correlation functions associated with each motion. The follow-

ing equation states the contribution of each of these motions:

$$\frac{1}{\tau_{\text{net}}} = \frac{1}{\tau_{\text{overall}}} + \frac{1}{\tau_{\text{local}}} \quad (10)$$

where  $\tau_{\text{overall}}$  corresponds to the overall tumbling of the entire chain or large segments of HTPB.  $\tau_{\text{local}}$  accords to segmental backbone rearrangements.  $\tau_{\text{net}}$  corresponds to the sum of all polymer motions. The correlation time,  $\tau_{\text{overall}}$ , for HTPB can be estimated from the following hydrodynamic equation<sup>44</sup>

$$\tau_{\text{overall}} = \frac{2M[\eta]\eta_0}{3RT} \quad (11)$$

where  $M$  is the molecular weight of HTPB.  $[\eta]$  is the intrinsic viscosity of the polymer solution in a given solvent with viscosity  $\eta_0$ .  $R$  is the gas constant.  $T$  is the absolute temperature. The viscosity of CDCl<sub>3</sub> at the room temperature is 0.54 cP. Hence,  $\tau_{\text{overall}}$  of 14.2 ns is obtained for HTPB. On the other hand, correlation times,  $\tau_{\text{local}}$ , are found to be on the order of tenth of a nanosecond. Then  $\tau_{\text{overall}}$  is between a hundred to a thousand times larger than  $\tau_{\text{local}}$ . Therefore,  $1/\tau_{\text{overall}}$ , compared to  $1/\tau_{\text{local}}$ , is negligible. This converts eq 10 to

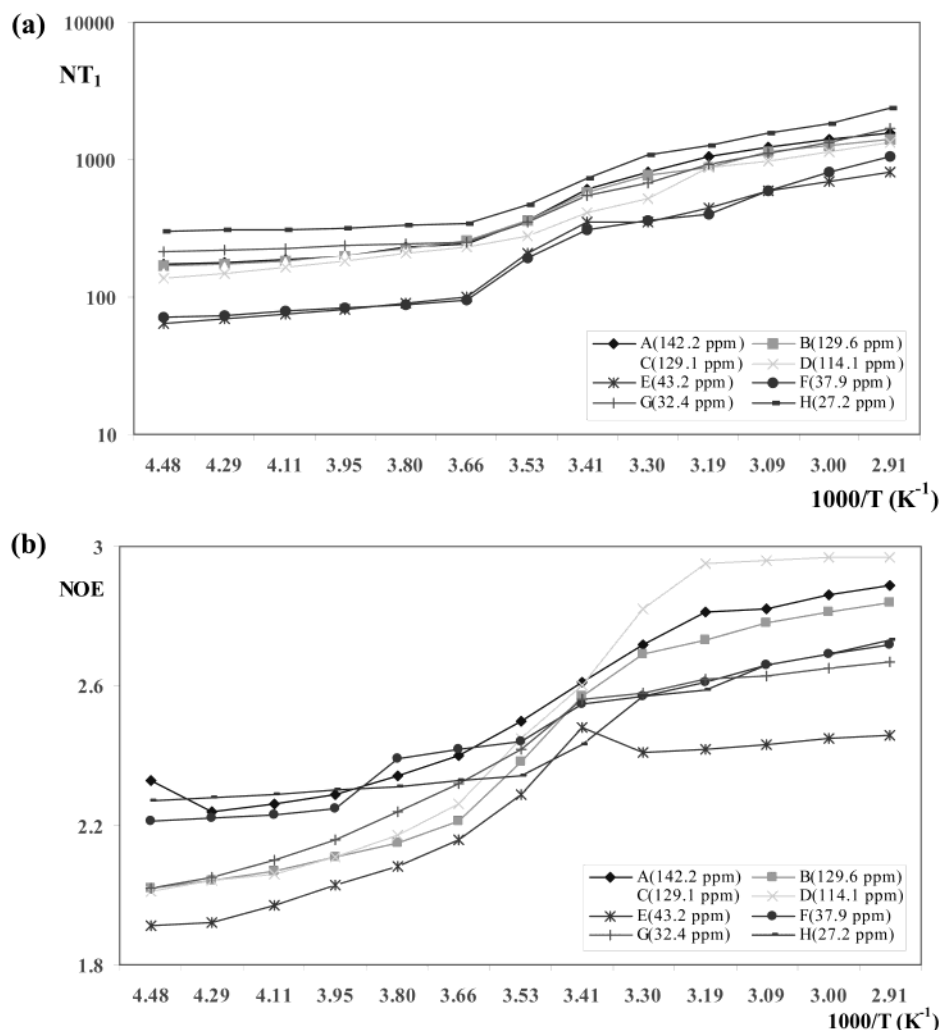


**Figure 3.** Experimental spin-lattice relaxation times,  $T_1$  (a), and NOE values (b) of protonated carbons of HTPB, as a function of temperature.

the following equation:

$$\tau_{\text{net}} \cong \tau_{\text{local}} \quad (12)$$

Hence, the overall motions of HTPB are much slower than the chain local motions and the former make negligible contributions to the relaxations of the backbone carbons. Therefore, relaxations and dynamics of HTPB may well be attributed to its local segmental motions.

The following conclusions are obtained through the measurements of temperature-dependent  $T_1$  and NOE relaxations and their corresponding correlation times.

The longest  $^{13}\text{C}$   $T_1$  value measured for HTPB is 2 s. This corresponds to the terminal methylene units of the polymer (63 ppm, Figure 1). The resonances of these units are so weak to obtain NOE data of any significance! Hence, calculations of its correlation times are merely possible through random isotropic tumbling model. This gives a  $\tau_c$  of 12 ps. Therefore, existences of strong intermolecular hydrogen bonds between polymer molecules appear less likely. Also, terminal methylenes seem to have a much higher motional freedom than those in typical alcohols and similar diols with shorter chains.

Olefinic vinyl methylenes, show a low  $T_1$  value (peak D, Table 1). A higher degree of freedom of motion is typically assumed for peripheral units. On this basis,

one expects a higher value of  $T_1$  for olefinic vinyl methylenes. Contrary to such expectations, low  $T_1$  values are observed! This is demonstrated by the low activation energy of 12.31 kJ/mol obtained, via the log  $\chi^2$  model (peak D, Table 2). This is the lowest activation energy encountered through this model.

Observed  $T_1$  order for aliphatic methylenes is  $\text{cis} > \text{trans} > \text{vinyl}$ . The order of corresponding correlation times is  $\text{cis} < \text{trans} < \text{vinyl}$ . These are calculated using the three dynamic models. Meanwhile, the calculated activation energy order is  $E_{a-\text{cis}} < E_{a-\text{trans}} < E_{a-\text{vinyl}}$ . This is obtained using log  $\chi^2$  distribution model. On the basis of these orders, one may conclude that concentration increase of vinyl form in the polymer reduces its mobility which induces its hardness and crystallinity while lowers its solubility. On the other hand, increase of the cis form in the polymer may increase its mobility, and consequently elasticity, softness and solubility.<sup>45</sup>

The ratio of average  $T_1$  values of the CH and  $\text{CH}_2$  groups,  $T_1(\text{CH})/T_1(\text{CH}_2)$ , is about 1.77 (Table 1). This value is different from 2, which is expected on the basis of the number of directly bonded protons. However, it is within the experimental error. On the other hand, the experimentally observed  $^{13}\text{C}\{^1\text{H}\}$  NOE values are also less than the ideal value (2.988). These reduced values suggest that segmental motions in HTPB are anisotropic.

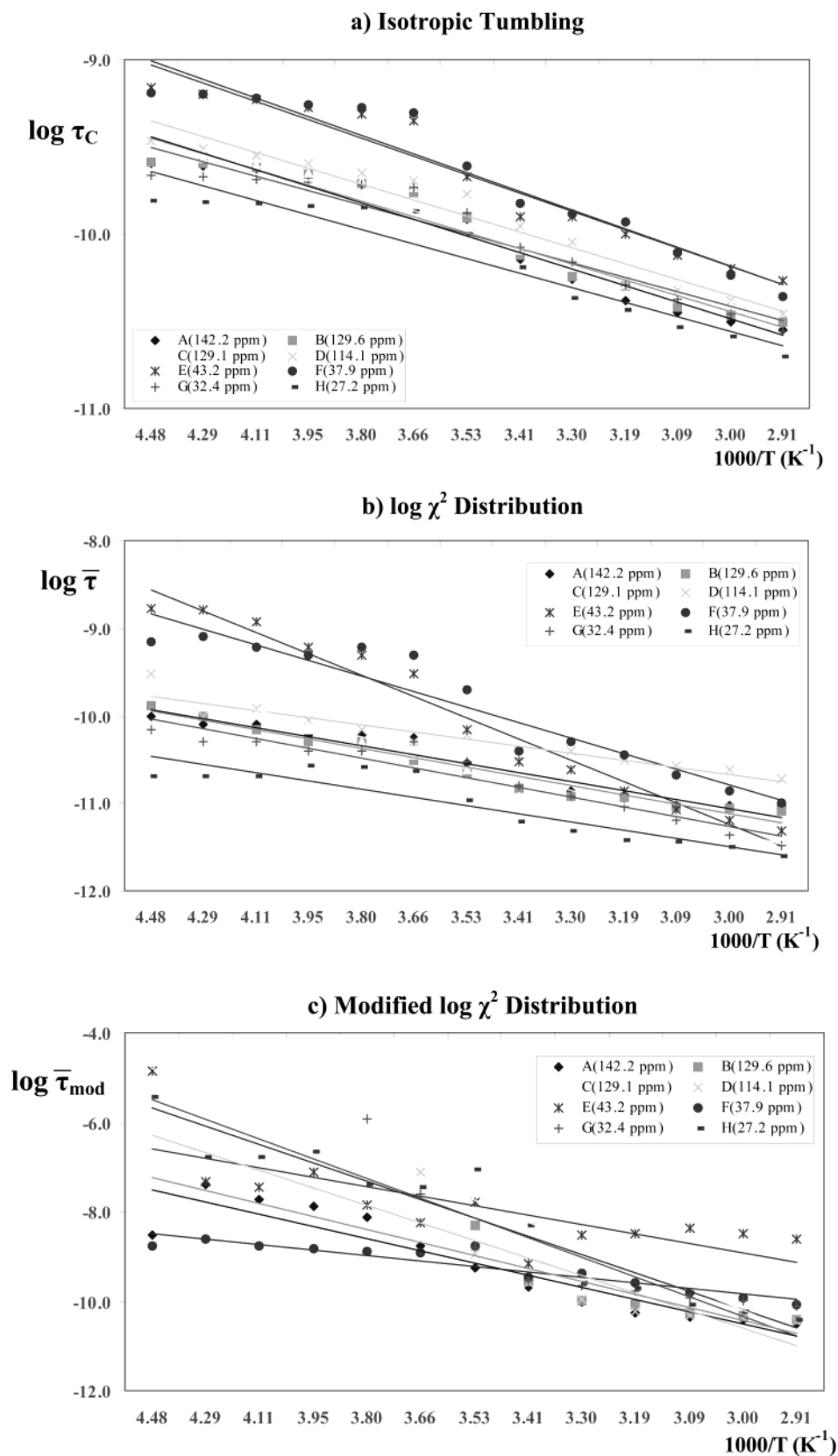


**Figure 4.** Logarithms of correlation times of protonated carbons of HTPB as a function of temperature, calculated by (a) the isotropic tumbling model, (b) the  $\log \chi^2$  distribution model and (c) the modified  $\log \chi^2$  distribution model.

$T_1$  and NOE values decrease as the temperature is lowered. Hence, the segmental motions of the polymer and  $T_1$  values decrease at lower temperatures. This means that the  $T_1$  minimum is lower than  $-50^\circ\text{C}$  and implies that the polymer is on the fast motion side of

the relaxation minimum. Also, all the three dynamic models employed, suggest that correlation times decrease as the temperature is increased. This is consistent with the increase of segmental motions as  $T_1$  or temperature is increased. Hence, the conformational



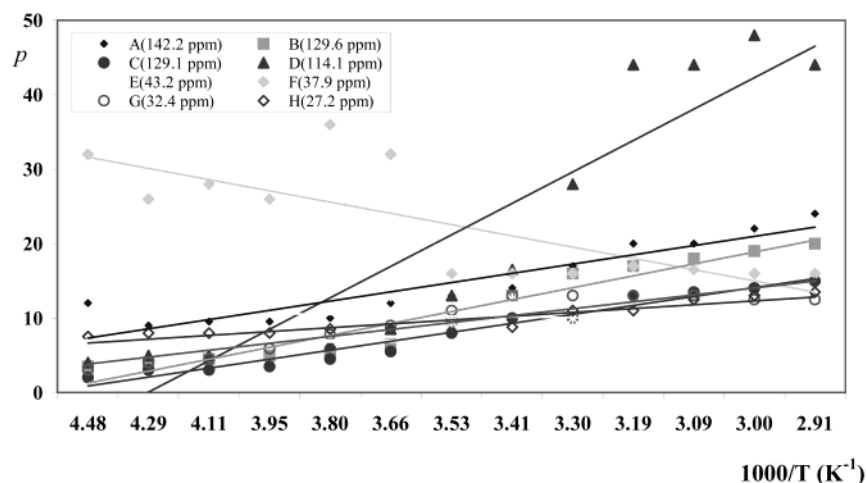


**Figure 5.** Calculated  $p$  as a function of temperature for protonated carbons of HTPB in accordance with the  $\log \chi^2$  distribution model (eq 8).<sup>36</sup>

changes of HTPB take place at a high frequency and speed while encountering low energy barriers. The magnitude of  $\tau$  is on the order of tenth of a nanosecond. Those of  $E_a$  are found to be in the range of kilojoules. The same ranges and trends of activation energies are reported for a different polybutadiene.<sup>46</sup> Calculated  $\tau$  values are rather small. This is consistent with the  $\tau_{\text{local}} \ll \tau_{\text{overall}}$  assumption.

Changes of the correlation times of the random isotropic tumbling vs temperature give a linear slope (Figure 4). This indicates that the random isotropic tumbling model shows similar activating energies for all the HTPB units. On the other hand, the modified  $\log \chi^2$  model of O'Connor and Blum<sup>11</sup> gives a rather exaggerating calculated values of  $E_a$  (Table 2). Therefore, the  $\log \chi^2$  distribution of Schaefer<sup>31</sup> appears to provide a more logical model for this case. Calculated  $p$  values increase as a function of temperature (Figure 5). A higher value of  $p$  is an indication of a higher degree of freedom. This justifies the observed dependence of  $p$  on temperature.

As NOE reaches its theoretical maximum value of  $\text{NOE}_{\text{max}} = 2.988$ , all dynamic models are expected to calculate similar correlation times. Nevertheless, the  $\log \chi^2$  distribution fails to meet such expectation. O'Connor and Blum's model of modified  $\log \chi^2$  distributions somehow overcomes the above discrepancy. However, at the vicinity of  $p = \ln b$  (here  $p = 6.9$ ) such calculations give unreasonable results (eq 9), while at  $p < 6.9$ , this model appears unapplicable.

Moreover,  $\bar{\tau}_{\text{mod}}$  goes to  $\bar{\tau}$  as  $p$  is increased. It is noteworthy that the  $\log \chi^2$  distribution model of Schaefer successfully describes dynamics of HTPB at the reduced NOE values. In short, it can be concluded that the  $\log \chi^2$  model of Schaefer is more successful in describing the dynamics of HTPB at reduced values of NOE, whereas the O'Connor and Blum model appears to offer a better description of HTPB dynamics at the NOE values that are close to the theoretical maxima.

## Conclusions

$T_1$  and NOE relaxations are measured for HTPB. This is done as a function of temperature ( $-50$  to  $+70$  °C), in  $\text{CDCl}_3$ . The relaxation data are interpreted in terms of chain local motions, using three dynamic models: (1) random isotropic tumbling, (2)  $\log \chi^2$  distribution, and (3) modified  $\log \chi^2$  distribution models. Among these, the

$\log \chi^2$  distribution model appears to be the most appropriate to describe the chain segmental motions of HTPB.

**Acknowledgment.** Special thanks go to Mr. H. R. Sannaee and Mr. M. Bassam at the Chemistry Department of Malek Ashtar University for their support and assistance. Also, we thank Mr. H. R. Bijanzadeh for his cooperation in NMR studies.

## References and Notes

- French, D. M. *Rubber Chem. Technol.* **1969**, *42* (1), 71.
- Heydari, H. M.S. Thesis. Tarbiat Modarres University, Tehran, 1995.
- Kassaei, M. Z.; Heydari, H. *Pittcon* **2001**.
- Booth, C.; Price, C., Eds.; *Comprehensive Polymer Science*; Pergamon Press: New York, 1990, Vol. 1; Chapter 17–19.
- Ibbett, R. N.; Ed.; *NMR Spectroscopy of Polymers*; Chapman & Hall: London, 1993.
- Karali, A.; Dais, P.; Heatley, F. *Macromolecules* **2000**, *33*, 5524.
- Smith, G. D.; Borodin, O.; Bedrov, D.; Paul, W.; Qiu, X.; Ediger, M. D.; *Macromolecules* **2001**, *34*, 5192.
- Sen, T. Z.; Bahar, I.; Erman, B.; Laupretre, F.; Monnerie, L.; *Macromolecules* **1999**, *32*, 3017.
- Liu, J.; Yee, A. F.; Goetz, J. M.; Schaefer, J. *Macromolecules* **2000**, *33*, 6853.
- Wu, J.; Xiao, C.; Yee, A. F.; Goetz, J. M.; Schaefer, J. *Macromolecules* **2000**, *33*, 6849.
- O'Connor, R. D.; Blum, F. D. *Macromolecules* **1994**, *27*, 1654.
- Heatley, F.; Spyros, A.; Dais, P. *Macromolecules* **1994**, *27*, 5845, 6207.
- Dais, P.; Radiotis, T.; Brown, G. R. *Macromolecules* **1993**, *26*, 1445.
- McBrierty, V. J.; Douglass, D. C.; Zhang, X.; Quinn, F. X.; Jerome, R. *Macromolecules* **1993**, *26*, 1734.
- Laupretre, F.; Bokobza, L.; Monnerie, L. *Polymer* **1993**, *34*, 468.
- Liang, M.; Blum, F. D. *Macromolecules* **1996**, *29*, 7374.
- Spyros, A.; Marchessault, R. H. *Macromolecules* **1996**, *29*, 2479.
- Jones, A. A.; Zhao, J.; Inglefeld, P. T.; Bendler, J. T. *Polymer* **1996**, *37*, 3783.
- Spera, S.; Po', R.; Abis, L. *Polymer* **1996**, *37*, 729.
- Blum, F. D. *Annu. Rep. NMR Spectrosc.* **1994**, *28*, 277.
- Dejean de la Batie, R.; Laupretre, F.; Monnerie, L. *Macromolecules* **1989**, *22*, 122, 2617.
- Dejean de la Batie, R.; Laupretre, F.; Monnerie, L. *Macromolecules* **1988**, *21*, 2045, 2052.
- Aspler, J. S. *Polym. Eng. Sci.* **1992**, *32*, 1379.
- Viovy, J. L.; Monnerie, L.; Brochan, J. C. *Macromolecules* **1983**, *16*, 1845.
- Weber, T. A.; Helfand, E. *J. Phys. Chem.* **1983**, *87*, 2881.
- Hall, C. K.; Helfand, E. *J. Chem. Phys.* **1982**, *77*, 3275.

- (27) Valeur, G.; Jarry, J. P.; Geny, F.; Monnerie, L. *J. Polym. Sci., Polym. Phys. Ed.* **1975**, *13*, 667, 675, 2251.
- (28) Jones, A. A.; Stockmayer, W. H. *J. Polym. Sci., Polym. Phys. Ed.* **1977**, *15*, 847.
- (29) Komoroski, R. A. *J. Polym. Sci., Polym. Phys. Ed.* **1979**, *17*, 45.
- (30) Heatley, F.; Begum, A. *Polymer* **1976**, *17*, 399.
- (31) Allerhand, A.; Doddrell, D.; Komoroski, R. *J. Chem. Phys.* **1971**, *55*, 189.
- (32) Doddrell, D.; Glushko, V.; Allerhand, A. *J. Chem. Phys.* **1972**, *56*, 3683.
- (33) Heatley, F. *Annu. Rep. NMR Spectrosc.* **1986**, *17*, 179.
- (34) Heatley, F. *Prog. Nucl. Magn. Reson. Spectrosc.* **1979**, *13*, 47.
- (35) McBrierty, V. J.; Douglass, D. C. *Phys. Rep.* **1980**, *63*, 61.
- (36) Schaefer, J. *Macromolecules* **1973**, *6*, 882.
- (37) Denault, J.; Morese-Seguela, B.; Seguela, R.; Prud'homme, J. *Macromolecules* **1990**, *23*, 4658.
- (38) Asakura, T. *Macromolecules* **1983**, *16*, 786.
- (39) Wittebort, R. J.; Sgabo, A.; Gurd, F. R. N. *J. Am. Chem. Soc.* **1980**, *102*, 5723.
- (40) Denault, J.; Prud'homme, J. *Macromolecules* **1989**, *22*, 1307.
- (41) Nagara, B.; O'Connor, R.; Blum, F. D. *J. Phys. Chem.* **1992**, *96*, 6417.
- (42) Blum, F. D.; Durairaj, B.; Padmanabhan, A. S. *Macromolecules* **1984**, *17*, 2837.
- (43) Craik, D. J.; Kumar, A.; Levy, G. C. *J. Chem. Inf. Comput. Sci.* **1983**, *1*, 30.
- (44) Riseman, J.; Kirkwood, J. G. *J. Chem. Phys.* **1949**, *16*, 442.
- (45) Kirk-Othmer *Encyclopedia of Chemical Technology*, 3rd ed.; John Wiley & Sons: New York, 1979; Vol. 8, p 548.
- (46) Gronski, M.; Quack, G.; Murayama, N.; Elgert, K. F. *Makromol. Chem.* **1975**, *176*, 3605.

MA030177O